Accepted Manuscript

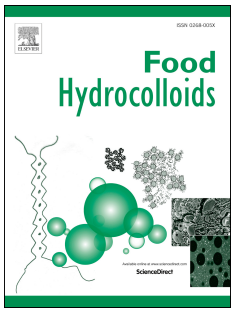

Structural and functional properties of OSA-starches made with wide-ranging hydrolysis approaches

Huaxin Han, Haixiang Zhang, Enpeng Li, Cheng Li, Peng Wu

PII: S0268-005X(18)31797-1

DOI: https://doi.org/10.1016/j.foodhyd.2018.12.011

Reference: FOOHYD 4815

To appear in: *Food Hydrocolloids*

Received Date: 16 September 2018

Revised Date: 3 November 2018

Accepted Date: 5 December 2018

Please cite this article as: Han, H., Zhang, H., Li, E., Li, C., Wu, P., Structural and functional properties of OSA-starches made with wide-ranging hydrolysis approaches, *Food Hydrocolloids* (2019), doi: https://doi.org/10.1016/j.foodhyd.2018.12.011.

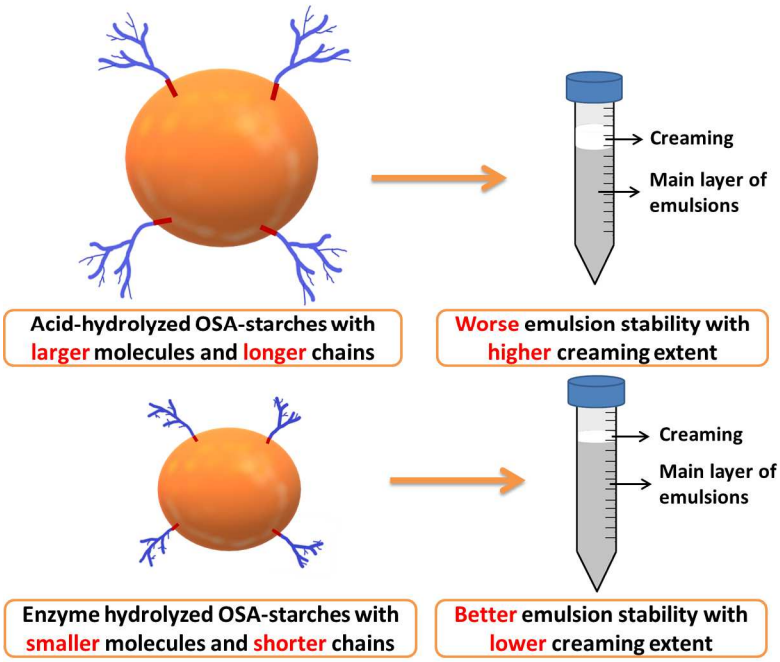

Structural and functional properties of OSA-starches made with wide-ranging hydrolysis approaches

Huaxin Han[a], Haixiang Zhang[b], Enpeng Li[a], Cheng Li[c] and Peng Wu[d, e*]

[a] Key Laboratory of Plant Functional Genomics of the Ministry of Education, Jiangsu Key Laboratory of Crop Genetics and Physiology, College of Agriculture, Yangzhou University, Yangzhou 225009, Jiangsu Province, China

[b] College of Life Science and Technology, Huazhong University of Science and Technology, Wuhan 430074, China

[c] Joint International Research Laboratory of Agriculture and Agri-Product Safety of Ministry of Education of China, Yangzhou University, Yangzhou 225009, Jiangsu Province, China

[d] Centre for Nutrition and Food Sciences, Queensland Alliance for Agriculture and Food Innovation, The University of Queensland, Brisbane, QLD 4072, Australia

[e] Suzhou Key Laboratory of Green Chemical Engineering, School of Chemical and Environmental Engineering, College of Chemistry, Chemical Engineering and Materials Science, Soochow University, Suzhou 215123, China

[*] Corresponding author:

Centre for Nutrition and Food Sciences, Queensland Alliance for Agriculture and Food Innovation, The University of Queensland, Brisbane, QLD 4072, Australia.

Email: p.wu@uq.edu.au or p.wu@suda.edu.cn

Phone: +61 7 3365 4809. Fax: +61 7 3365 118

Abstract

Octenyl succinic anhydride modified starches (OSA-starches) are widely used as emulsifiers and stabilizers in the food industry. This study investigates the relationships between molecular structure and emulsifying and antioxidant properties of OSA-starches with a wide range of structures, formed by hydrolysis by α-amylase, β-amylase and HCl for various hydrolysis times. Structural parameters, namely molecular size distribution, chain-length distribution, degree of branching (DB) and degree of OSA substitution (DS) were characterized using size-exclusion chromatography and ^{1}H nuclear magnetic resonance. These parameters were then correlated with viscosity, emulsification performance and antioxidant properties for OSA-stabilized oil emulsions, to gain improved understanding of structure-property relationships. The average chain length (DP) and DB respectively showed positive and negative correlations with the viscosity, total antioxidant activity (TAC), creaming extent and the emulsion z-average droplet size for all the hydrolyzed samples. The OSA-starches treated by α-amylase generally had the smallest average DP and largest DB, resulting in the lowest viscosity and the best droplet stability with the smallest creaming extent. The acid-hydrolyzed OSA-starch samples presented larger average DP than the enzyme-hydrolyzed samples, in agreement with their better TAC, while larger creaming extent. The β-amylase-hydrolyzed samples produced moderate structural degradation and emulsifying properties compared to the OSA-starches treated by α-amylase and HCl. The structure-property correlations indicate that the

average chain length and DB are the two most important structural parameters in determination of the functional properties for the OSA-modified starches. These findings will help develop improved food additives with desired functions.

Keywords: OSA starch, starch hydrolysis, antioxidant, SEC, emulsification, structure-property relations

Chemical compounds studied in this article

Octenyl succinic anhydride (PubChem CID: 5362721); Medium chain triglyceride (PubChem CID: 93356)

Abbreviations

CLD, chain-length distribution; DMSO, dimethyl sulfoxide; DP, degree of polymerization; DB, degree of branching; DS, degree of substitution; FRAP, ferric reducing antioxidant power; MCT, medium chain triglyceride; NMR, nuclear magnetic resonance; OSA, octenyl succinic anhydride; RID, refractive index detector; SEC, size-exclusion chromatography; TAC, total antioxidant capacity.

1. Introduction

Starch (a large complex branched glucose polymer) modified with octenyl succinic anhydride (OSA) is often used to produce compounds such as emulsion stabilizers and encapsulating agents, especially as food additives. After OSA modification, the normally hydrophilic starch gains a hydrophobic element in the form of octenyl groups, resulting in large molecules with an amphiphilic character. When adsorbed onto an emulsion droplet, the hydrophilic carboxylic acid groups extend in the aqueous phase, the hydrophobic octenyl chain goes into the oil, while the complex polysaccharide forms a dense, continuous, thick interface membrane at the oil-water interface (Mortenson & Reineccius, 2008; Sweedman, Hasjim, Tizzotti, Schaefer, & Gilbert, 2013), which functions as a complex branched colloidal stabilizer (Napper, 1983; Tesch, Gerhards, & Schubert, 2002). This membrane structure has a strong steric hindrance effect, as well as electrostatic repulsion from the carboxylate groups (depending on the pH). This gives electrosteric colloidal stabilization so that the droplets do not aggregate easily (Modig, Nilsson, Bergenståhl, & Wahlund, 2006; Zhang et al., 2018). OSA-starches are widely used as additives in the food industry, and good antioxidant activity is highly desirable (Park, Chung, & Yoo, 2004).

Starch molecular structure plays a significant role in determining the functional properties of OSA starches. A number of studies have been carried out to investigate the relationships between starch structure and emulsifying properties of OSA starches. For example, OSA-starches with lower molecular weight tend to have higher

encapsulation efficiency and capacity (Hategekimana, Masamba, Ma, & Zhong, 2015), while OSA-starch samples containing larger molecules have better emulsion stability (Dokic, Dokic, Dapcevic, & Krstonosic, 2008; Nilsson & Bergenståhl, 2006). Rigid macromolecules with higher degree of branching, DB, can lead to more stable emulsion due to steric effects (Sweedman, Schaeffer, & Gilbert, 2014), but DB itself is less influential than the molecular size and branching chain length for the degraded starches (high DB value) and linear molecules (low DB value) (Liu et al., 2008). Moreover, the degree of substitution (DS) plays an important role in determination of OSA-starches emulsion properties (Liu et al., 2008; Nilsson et al., 2006; Nilsson & Bergenståhl, 2007). The emulsifying capacity and emulsion stability can be improved with increasing DS values (Nilsson et al., 2007; Wang, Su, & Wang, 2010). Higher DS and larger molecules with more branches can better stabilize oil droplets (Nilsson et al., 2007; Sweedman, Hasjim, Shaefer, & Gilbert, 2014).

The molecular structure of OSA starches can be controlled both through the structure of the parent starch and through chemical modification prior to or during the addition of OSA to the parent starch. For instance, β-amylase specifically cleaves (1→4)-α glycosidic bonds from the non-reducing ends of starch branches, releasing a maltose for each successful hydrolysis (Xu, Huang, Fu, & Jane, 2015) while α-amylase is an endo-amylase which also only cuts (1→4)-α bonds, with the hydrolysis occurring randomly in the interior of starch chains (Dhital, Warren, Butterworth, Ellis, & Gidley, 2017; LeCorre, Vahanian, Dufresne, & Bras, 2012). Acid is usually used to degrade

104 starch granules rather than gelatinized starch, which can hydrolyze both (1→4)-α and
105 (1→6)-α bonds (Hoover, 2000; Wang, Blazek, Gilbert, & Copeland, 2012). Starch
106 structural parameters, such as starch molecular size, chain-length distribution (CLD)
107 and DB, can be changed with enzymatic or acid treatment, resulting in functional
108 changes of the OSA starches. However, how the structural changes of the OSA starches
109 induced by enzymes and acid treatment affect their functional properties remains
110 unclear. The correlations between the structural parameters and the physico-chemical
111 properties are still far from exhaustively investigated.

112 In our previous work, the structural and emulsifying properties of a range of
113 commercial OSA modified starches produced by the three different degrading
114 treatments (α-amylase, *β*-amylase and HCl) were examined (Zhang et al., 2018).
115 However, there was no systematic variation in hydrolyzing procedures such as
116 hydrolysis time and enzymatic concentration, which limited the “space” of molecular
117 structures; a wide range of structures is desirable to obtain and understand structure-
118 property relations. Moreover, the total antioxidant capacity (TAC), which plays a key
119 role in human health, of these commercial OSA-starch samples was not measured in
120 that study. In the current study, the OSA waxy maize starches were prepared and then
121 used for hydrolysis tests with different treatments (hydrolyzed by *α*-amylase, *β*-
122 amylase and HCl for different time periods). The molecular structures of the
123 hydrolyzed products, both whole and debranched, were characterized using size-
124 exclusion chromatography (SEC, a type of gel-permeation chromatography, GPC).

Functional properties, including emulsification properties and TAC, of the hydrolyzed OSA-starches were also determined. The structure-property correlations were analyzed to study the in-depth relationships between the structure and functions of the OSA starches, as well as to explore possible approaches to obtaining samples with suitable properties in the future.

2. Materials and methods

2.1. Materials

Waxy maize starch was provided by Lihua Company (Qinhuangdao, China). Medium chain triglyceride (MCT) was purchased from Houman Biological Tech. Co., LTD (Shanghai, China). 2-Octen-1-ylsuccinic anhydride (OSA, 97%), trifluoroacetic acid-d_1 (TFA-d_1), β-amylase (from barley, type II-B, 41.6 units/mg), α-amylase (from porcine pancreas, Type VI-B, ≥10 units/mg solid) and LiBr were all purchased from Sigma-Aldrich Chemical Co. (St. Louis, MO, USA). Trolox and the FRAP assay kit were purchased from the Beyotime Institute of Bio-technology (S0116, Nantong, China). Perdeuterated dimethyl sulfoxide (DMSO)-d_6 was purchased from Cambridge Isotope Laboratories, Inc. (Tewksbury, MA, USA). DMSO (GR) was purchased from Meck & Co., Inc. (Kenilworth, NJ, USA). Other chemical reagents were analytical grade and used as received.

2.2. Preparation of OSA-starches

Native starch granules were modified with OSA following published methods with

minor modifications (LeCorre et al., 2012; Sweedman et al., 2014; Viksø-Nielsen, Andersen, Hoff, & Pedersen, 2006; Wang et al., 2012). Waxy maize starch (500 g) was suspended in distilled water (750 mL) and then the pH of the suspension was maintained at 8.5 with 0.2 M NaOH during the reaction. OSA (15 g, dissolved in 30 g ethanol; 3% on the basis of dry starch weight) was added drop-wise over 3 h to the suspension with continuous stirring at 35^{o}C, followed by incubating for 1 h. At the end of the reaction, the suspension was neutralized with 0.1 M HCl. The resultant starch suspension was washed twice with ethanol to remove the residual reagents, and dried overnight at 50^{o}C in an oven for later use.

2.3. Hydrolysis of the OSA-starch samples

2.3.1. Acid hydrolysis

Acid hydrolysis of the OSA-starch samples was carried out based on the method of Robyt, Choe, Hahn, and Fuchs (1996). Briefly, the OSA-starch (50 g, dry basis) was hydrolyzed in batches with 2.2 M HCl at 35^{o}C (1.0 g starch/5 mL acid solution) for periods ranging from 3 to 336 h (3, 6, 12, 24, 72, 120, 168, 336 h). The slurries were then neutralized with 2 M NaOH at the termination of each hydrolysis period. The collected granular residues were treated using vacuum filtration method by washing once with deionized water and twice with ethanol. The rinsed starch granules were collected and freeze-dried for later structural and functional analyses.

2.3.2. Hydrolysis by β-amylase

165 The hydrolysis of the OSA-starch samples with *β*-amylase was performed by the
166 method of Sweedman, Tizzotti, Schafer, and Gilbert (2013). A sample of 50 g dry
167 OSA-starch was dispersed in distilled water to achieve a dry matter content of 14%
168 (w/w) and its pH was adjusted to 5.5 using 0.2 M HCl, followed by gelatinizing in a
169 boiling water bath for 1 h. After cooling down to 45^{o}C, the gelatinized OSA-starch
170 samples were hydrolyzed in batches with 5 mL sodium acetate (0.01 M, pH=5.5)
171 containing three different concentrations of enzyme (high: 1 mg/g starch; medium: 0.2
172 mg/g starch; low: 0.1 mg/g starch) for 0.5, 1, 2 and 4 h at 45^{o}C. The pH of the
173 hydrolysates was adjusted to 12 to deactivate enzyme at the end of each hydrolysis
174 period with continuous stirring at 300 rpm for 20 min, followed by neutralizing with 1
175 M HCl. The *β*-amylolysis hydrolysates with different hydrolysis times were collected
176 and immediately freeze-dried for later use.

177 *2.3.3. Hydrolysis by α-amylase*

178 The OSA-starch sample (50 g) was dispersed in distilled water (14%, w/w, dry
179 matter) and the mixture was adjusted to pH 6.8 (using 1 M HCl) followed by keeping
180 in a boiling water bath for at least 1 h. The gelatinized starch was then cooled to 37^{o}C.
181 The *α*-amylolysis of the OSA-starch was performed in batches at 37^{o}C in a 2 L beaker
182 containing 5 mL *α*-amylase solution and 5 mL $CaCl_2$ solution as enzyme promoting
183 agent (Viksø-Nielsen et al., 2006) for 30-240 min. The *α*-amylase solution was
184 prepared by dissolving *α*-amylase (2 mg/g starch) in 5 mL phosphate buffer solution
185 (0.2 M, pH 6.8). At the end of each hydrolysis period, the hydrolysates were adjusted

186 to pH=12 for enzyme denaturalixation with 2 M NaOH and then neutralized with 1 M
187 HCl. The *α*-amylolysis hydrolysates with varying hydrolysis times were stored at -
188 20^{o}C and freeze-dried for later use.

189 ***2.4. Characterization of structural features***

190 *2.4.1. Debranching of hydrolyzed OSA-starch samples*

191 This procedure is to obtain the CLD: the number of chains as a function of their
192 degree of polymerization. Approximately 4-6 mg of each OSA-starch sample after the
193 treatments with HCl, *α*-amylase or *β*-amylase were debranched using isoamylase
194 following a method described previously (Tran et al., 2011) with slight modifications.
195 In brief, the starch sample was dissolved with 0.9 mL of deionized water in a boiling
196 water bath for 30 min, followed by cooling to room temperature. Next, sodium azide
197 solution (5 μL, 0.04 g/mL) and 100 μL sodium acetate buffer (0.1 M, pH 3.5) were
198 added to the starch suspension before the addition of 2.5 μL isoamylase solution. The
199 mixture was incubated in a water bath at 37^{o}C for 3 h. Next, 0.1 M NaOH was added
200 drop-wise to increase the pH to 7, followed by heating to 80^{o}C for 1 h, and then
201 centrifuged at 4000 g for 10 min. The supernatant containing debranched starch was
202 frozen in liquid nitrogen before being freeze-dried overnight. For the purpose of
203 comparison, the structures of the whole and debranched non-hydrolyzed OSA-starch
204 (OS) were also characterized.

205 *2.4.2. Starch structural characterization using SEC*

206 Whole and debranched hydrolyzed OSA-starch samples were dissolved in dimethyl

sulfoxide (DMSO) with 0.5% (w/w) LiBr overnight at 80°C to yield a final concentration of 2 mg/mL and 4 mg/mL, respectively. The whole molecular size and the CLDs were analyzed using an Agilent 1260 Infinity SEC system (Agilent, Santa Clara, CA, USA) equipped with a refractive index detector (RID, Optilab UT-rEX, Wyatt, Santa Barbara, CA, USA). A series of PSS separation columns consisting of GRAM Pre-Column, GRAM 100 and 1000 analytical columns (Polymer Standards Service, Mainz, Germany) placed in an oven at 80°C were used for both the whole and debranched samples. The volume of each injection was 100 μL, and DMSO containing 0.5% (w/w) LiBr was used as eluent with a flow rate of 0.3 and 0.6 mL/min for whole and debranched starch characterizations, respectively. Pullulan standards with known peak molecular weights ranging from 342 to 2.35×10^6 Da were used for calibration to obtain a relationship between SEC elution volume and the hydrodynamic volume (the SEC size separation parameter, the hydrodynamic volume V_h, or the corresponding radius, R_h) of starch molecules using the Mark–Houwink relation (Vilaplana & Gilbert, 2010a). The Mark-Houwink parameters K and α of pullulan in DMSO/LiBr solution at 80°C are 2.424×10^{-4} dL/g and 0.68, respectively (Cave, Seabrook, Gidley, & Gilbert, 2009). Considering the possible shear molecular degradation for large-size molecules such as amylopectin during separation using SEC, the whole starch molecular size should be presented apparently. The size distributions of the smaller chains (the "amylose" region and debranched amylopectin) can be reliably obtained essentially free of shear-scission artefacts (Cave et al., 2009). For linear molecules (such as

228 debranched starches), the R_h of debranched starch can be converted to X, the degree of
229 polymerization (DP) through the Mark-Houwink relation. The average chain length ($\bar{X}$)
230 is calculated from the chain-length distributions (CLDs) of debranched SEC as
231 described previously (Vilaplana et al., 2010a).
232
233 *2.4.3. Determination of DB and DS using NMR*
234 The ^{1}H NMR spectra of the hydrolyzed OSA-starches were obtained using a
235 previously described method (Tizzotti, Sweedman, Tang, Schaeffer, & Gilbert, 2011).
236 Approximately 3 mg of each OSA-starch after hydrolysis was dissolved in 0.5 mL
237 DMSO-d_6 overnight at 80^{o}C. TFA-d_1 (~20 mg) was added to the sample medium
238 before analysis to shift the starch OH groups and water signals toward higher chemical
239 shifts. The NMR spectra was measured at 50^{o}C on an NMR spectrometer (Agilent,
240 USA), operating at an observation frequency of 399.82 MHz for ^{1}H, equipped with an
241 OneNMR probe (Agilent) (8.40 μs 90^o pulse, a repetition time of 4.556 s composed of
242 an acquisition time of 2.556 s and a relaxation delay of 2 s, 128 scans. The DB and DS
243 were obtained as described in detail elsewhere (Tizzotti et al., 2011).

244 ***2.5. Evaluation of functional properties of the hydrolyzed OSA-starch samples***
245 *2.5.1. Apparent viscosity*
246 The OSA-starch samples after hydrolysis were mixed with hot water (40%, w/w,
247 dry matter) and kept in a 50°C water bath for overnight. The viscosity of the mixture
248 was measured using a rotational viscometer (NDJ-5S, Shanghai Changji Geological

Co., Ltd, Shanghai) with a small sample adapter. The tests were carried out at 50°C with a spindle No. 21 at a speed of 60 rpm (Zhang et al., 2018).

2.5.2. Emulsion preparation

The emulsion was prepared as described previously (Stang, Schuchmann, & Schubert, 2001; Zhang et al., 2018). Firstly, deionized water was added for dispersion of the hydrolyzed OSA-starch samples (14 g, pH=7) to achieve a dry matter content of 40%, followed by addition of medium chain triglycerides (MCT, 15% w/w, based on the mass of OSA-starch dispersion) and sodium azide solution (0.5% w/w, 0.04 g/mL). The mixture was homogenized at 28000 rpm for 5 min using a homogenizer (XHF-D, Ningbo Scientz Biotechnology Co., Ltd, Ningbo, China) to obtain an initial emulsion, then processed with a high pressure homogenizer (JN-02HC, Guangzhou Juneng Biotechnology Co., Ltd, Guangzhou) under 400 bar for six cycles at 30°C to obtain a final emulsion. The emulsions were sealed in tubes and stored away from light at room temperature for 0, 48 and 168 h to measure the emulsion stability. The amount of OSA starch in the emulsion was always well above the critical aggregation concentration for such samples (Tizzotti, Sweedman, Schaefer, & Gilbert, 2013), and thus emulsifier aggregates (polydisperse micelles) may be present, even though much of the emulsifier would be adsorbed onto the droplets.

2.5.3. Emulsion droplet size and stability

The droplet size of the emulsions was determined using dynamic light scattering

(DLS) with a Malvern Zetasizer Nano (ZS90, Malvern Instruments Ltd, Worcestershire, UK). The refractive indices of the MCT and water were taken as 1.414 and 1.330, respectively, and the adsorption index as 0.001 (Zhang et al., 2018). A small drop of the emulsion was taken out and diluted approximately 500 × by distilled water before testing. The droplet size of each sample was tested at 3 different time points, immediately after emulsification (0 h), at 48 and at 168 h. After a relatively long storage time (i.e. over 24 h), some creaming (emulsion-breaking) was observed on the top layer of the emulsions, most particularly for the acid and *β*-amylase hydrolyzed OSA-starch samples. The height of the creamed layer at the top of the centrifuge tube and the total height of the emulsion sample were measured with a ruler, to give the creaming extent as the ratio of the height of creamed layer to the total emulsion. The stability of the uncreamed part of the emulsions was measured from the change of droplet size with storage time. All measurements were performed at 25°C for at least three separately prepared samples.

2.5.4. Total antioxidant capacity

The total antioxidant capacity (TAC) of all the hydrolyzed OSA-starch samples and OS was determined following a previously described method (Luo, Li, & Kong, 2012). The TAC was represented by ferric reducing antioxidant power (FRAP), which was assayed according to instructions from Beyotime Institute of Biotechnology. Stock solutions including detective buffer, TPTZ (2,4,6-s-triazine) solution, TPTZ dilution, 0.5 mL 10 mM $FeSO_4$ solution and 0.1 mL 10 mM Trolox solution were prepared. The

fresh FRAP working solution was prepared by mixing TPTZ dilution, detective buffer and TPTZ solution in a ratio of 10:1:1 (v/v) and heated to 37°C before use. A sample of the hydrolyzed OSA-starch samples (4 mg) was dissolved in 1000 μL distilled water at 80°C for at least 2 h (Benzie & Strain, 1996). Next, 5 μL of the solution was withdrawn and mixed with 180 μL of the FRAP working solution and then kept at 37°C for 5 min. The absorbance of the reaction mixture was then recorded at 593 nm using a UV spectrophotometer. The standard curve was prepared using $FeSO_4$ solutions ranging from 0.15 to 1.5 mM. The TAC was expressed by $FeSO_4$ values, calculated using the standard curves.

2.6. Statistical analysis

All determinations of the structural measurements were performed in duplicate and the analyses of the functional properties were conducted in triplicate. The results were expressed as mean ± standard deviation. Pearson and Spearman correlation analyses were carried out using IBM SPSS Statistics. Statistical significance was set at $p = 0.05$.

3. Results and discussion

3.1. Structures of the hydrolyzed OSA-starch samples

3.1.1. Whole molecular size distribution

These are measured as the SEC weight distribution w (logR_h), which is the weight (not molecular weight) of whole molecules as a function of hydrodynamic radius (R_h). As shown in Fig. 1 for all OSA-starch samples after the hydrolysis treatments with α-

amylase (a), β-amylase (b) and HCl (c), the apparent whole molecular size was significantly reduced compared to the non-hydrolyzed OSA-starch (OS) and always decreased with the increase of hydrolysis time. The β-amylase hydrolyzed OSA-starch samples (Fig. 1b) generally had two peaks ranging from R_h ~ 0.3 nm to ~ 300 nm in the apparent whole starch size distributions, and the dextrin fractions showed some significant differences in their size distributions. The average molecular size, $\overline{R_h}$ (Vilaplana & Gilbert, 2010b), decreased significantly with the increase of hydrolysis time and the enzyme concentration (Table 2), indicating the molecular degradation of the OSA-starches. For example, the $\overline{R_h}$ of the OSA-starch was reduced from the initial 80.6 nm (OS) to 36.6 nm after 0.5 h hydrolysis with β-amylase at the enzyme concentration of 0.1 mg/g starch (BL0.5), and then decreased to 2.4 nm after 2 h hydrolysis at 1 mg/g starch (BH2). A strong peak was observed for all β-amylase hydrolyzed OSA-starch samples, particularly for BH1 and BH2, at R_h ~ 0.4 nm, which are thought to be maltose fractions (Fig. 1b). Similar results were also reported previously (Zhang, et al., 2018). Similar molecular degradation was found for the OSA-starch samples with α-amylase and HCl treatments (Fig. 1a and Fig. 1c, respectively). However, the features of the chromatographic profiles are different in terms of the peak position, shape and size. Moreover, the size distributions for the acid-hydrolyzed OSA-starch samples (Fig. 1c) were a little narrower than those of the enzyme-hydrolyzed samples (Fig. 1a and Fig. 1b), as acid is able to penetrate more deeply into starch granules and thus cleave more randomly than enzyme (Ma & Robyt,

1987). In addition, it took up to 336 h to achieve a final $\overline{R_h}$ of ~ 3 nm using the acid hydrolysis method, whereas it just required a few hours to reach the same hydrolysis extent using the enzyme hydrolysis methods. This suggests the significantly higher hydrolysis efficiency of the enzymes.

Table 1. All structural and functional parameters of the OSA-starch samples after hydrolysis with α-amylase, *β*-amylase and HCl for different periods of time[1, 2, 3]

Hydrolysis approach	Sample name	Structural parameters				Functional parameters									
		$\overline{R_h}$ /nm	$\bar{X}$	DB /%	DS	Antioxidant /mM	Viscosity /mPa.s	Creaming extent (168 h)		z-average droplet size/nm			Droplet stability			
													%		%/h	
								%	%/h	0 h	48 h	168 h	48 h	168 h	48 h	168 h
	OS	80.6	22.3	3.6	0.027	NA	3918	NA	NA	NA	NA	NA	NA	NA	NA	NA
α-amylase	A0.5	24.0	11.0	5.3	0.027	0.189	25	6.9	0.04	405	418	438	3.2	8.1	0.07	0.05
	A1	8.0	8.2	5.5	0.029	0.187	23	7.7	0.05	360	375	397	4.2	10.3	0.09	0.06
	A1.5	5.7	7.3	5.4	0.028	0.198	20	7.1	0.04	366	358	393	2.1	7.4	0.04	0.04
	A2	4.8	6.6	5.6	0.026	0.196	19	7.4	0.04	311	323	324	3.8	4.2	0.08	0.03
	A3	3.8	5.7	5.9	0.027	0.207	14	7.3	0.04	272	285	298	4.8	9.6	0.10	0.06
	A4	3.4	5.2	6.0	0.027	0.198	13	6.9	0.04	241	241	262	0.2	8.6	0.00	0.05
β-amylase	BL0.5	36.6	15.9	4.1	0.036	0.298	2695	12.3	0.07	459	478	524	4.1	14.2	0.09	0.08
	BL1	23.5	15.1	4.6	0.034	0.307	1328	13.7	0.08	365	412	432	12.9	18.4	0.27	0.11
	BL2	17.3	14.1	4.3	0.028	0.298	1133	13.4	0.08	308	345	364	12	18.2	0.25	0.11
	BL4	8.2	10.2	4.5	0.028	0.306	112	13.7	0.08	244	296	305	21.4	25.2	0.45	0.15
	BM2	6.9	8.6	4.6	0.028	0.337	53	14.0	0.08	227	278	322	22.5	41.0	0.47	0.24
	BH0.5	3.8	6.4	5.3	0.029	0.322	16	12.7	0.08	221	226	244	2.3	10.4	0.05	0.06
	BH1	2.9	5.1	6.0	0.03	0.36	9	13.0	0.08	204	231	244	13.2	19.6	0.28	0.12
	BH2	2.4	4.8	6.3	0.031	0.455	6	13.1	0.08	197	229	233	16.1	18.3	0.34	0.11
HCl	H3	24.0	18.0	4.1	0.03	0.641	1187	13.9	0.08	519	538	553	3.8	6.6	0.08	0.04
	H6	23.4	17.8	4.3	0.029	0.579	610	14.9	0.09	684	746	827	9	20.9	0.19	0.12
	H12	27.9	17.5	4.4	0.026	0.719	420	14.4	0.09	567	577	633	1.8	11.6	0.04	0.07
	H24	11.5	16.8	4.6	0.015	0.741	42	14.6	0.09	264	311	362	17.7	37.1	0.37	0.22
	H72	4.6	15.2	4.7	0.01	0.624	27	20.1	0.12	376	NA	NA	NA	NA	NA	NA
	H120	2.8	13.6	4.9	0.009	0.706	25	25.2	0.15	335	NA	NA	NA	NA	NA	NA
	H168	3.4	14.1	5.2	0.009	0.756	21	28.1	0.17	300	NA	NA	NA	NA	NA	NA
	H336	3.0	13.0	5.7	0.007	0.719	31	33.3	0.20	272	NA	NA	NA	NA	NA	NA

[1] "NA" for the OS (non-hydrolyzed OSA-starch) means that the emulsifying properties for the OS could not be measured because the OS was too viscous after gelatinization to be completely homogenized, which resulted in the failure of the preparation of emulsion. The total antioxidant capacity (TAC) of the

OS was too low and thus not included here. "NA" for the samples of H72, H120, H168 and H336 means the emulsion droplet size after 48 h could not be tested due to the gelation effect after emulsification

[2] The sample code OS is non-hydrolyzed OSA-starch; other codes are the same as shown in **Fig. 1.**

[3] The creaming extent is presented in two forms: 1) the creaming ratio (%) of the height of the creamed layer at the top of the centrifuge tube and the total height of the emulsion sample at t=168 h; 2) the time evolution of the creaming ratio denoted by the average creaming ratio per hour (%/h). Similarly, the droplet stability is also presented in two forms: 1) the change (%) in the droplet size of the emulsions over storage with respect to the droplet size of the fresh emulsion; 2) the time evolution of the droplet size change (%/h).

3.1.2. Chain length distribution of debranched starch

Fig. 2 shows the weight chain-length distributions (CLDs) of the OSA-starches after being hydrolyzed by α-amylase (a), β-amylase (b) and HCl (c) for different times, with two peaks observed in general. With the increase of hydrolysis time, the average chain length, $\bar{X}$, was significantly decreased irrespective of the hydrolysis methods (Table 1). The CLDs of OSA-starches could be affected significantly by the hydrolyzing processes as well as the molecular structures of parent starches (Lin, Lee, & Chang, 2003; Sweedman et al., 2013; Zhang et al., 2018). The type of starch used in current research was waxy maize starch. So the differences in the CLDs among these samples are ascribed to the varying hydrolysis approaches. As presented in Fig. 2b, all the β-amylase hydrolyzed OSA-starch samples had a maltose peak and the peak height increased with the increasing hydrolysis time, in line with the results of the whole molecular size distributions (Fig. 1b). Compared with the enzyme-treated

363 OSA-starches, the acid-hydrolyzed samples had a narrower CLD, which is also
364 consistent with the whole molecular size distribution results (Fig. 1c).

365 For the samples prepared either using acid or enzyme hydrolysis, the degradation
366 mainly happens in the amorphous region (Miao, Li, Huang, Jiang, & Zhang, 2015;
367 Sweedman, Hasjim et al., 2014), while the crystalline region was degraded slowly.
368 Even after several days of acid hydrolysis, the short chains of OSA-starch were well-
369 preserved (Fig. 2c). α-amylolysis and β-amylolysis samples showed degradation of
370 amylopectin branch chains with the increase of hydrolysis time and enzyme
371 concentration (Fig. 2a and b), as the OSA-starch samples were gelatinized before
372 enzyme treatment. As a result, the chain length of the enzyme-hydrolyzed OSA-starch
373 samples was reduced to a larger extent and at a faster rate compared to those of the
374 acid-hydrolyzed samples.

375 *3.1.3. Degree of branching*

376 DB of OSA-modified starch is an important factor for the stabilization of
377 emulsions, because more branched samples are more likely to be better steric
378 stabilizers (Sweedman, Hasjim et al., 2014; Sweedman, Schaeffer et al., 2014). The
379 NMR spectra of representative samples treated by α-amylase, β-amylase and HCl are
380 shown in Fig. SI of Supporting Information. The DBs of the OSA-starch samples,
381 calculated from the spectra as described previously (Tizzotti et al., 2011), are shown

382 in Fig. 3. Compared to the non-hydrolyzed OSA-starches (OS), the DB values of all
383 the hydrolyzed samples were higher and generally increased with increasing
384 hydrolysis time and/or enzyme concentration. This is particularly for the *β*-amylase
385 hydrolyzed samples (Fig. 3b) having more (1→4)-α linkages, have higher
386 probabilities of being cleaved by enzymes (Hamaker, Lee, & Quezada-Calvillo,
387 2012). Note that *α*-amylase is an endo-amylase which only cuts (1→4)-α linkages, but
388 the hydrolysis occurs randomly in the interior of starch chains. Thus the DB values of
389 the *α*-amylase hydrolyzed OSA-starch samples only slightly increased with the
390 increase of hydrolysis time. Similar results are observed for the acid-treated samples
391 (Fig. 3c).

392 *3.1.4. Degree of substitution*

393 The DS of OSA-starches, giving the relative amounts of the hydrophobic units
394 and the ionizable units, is a key factor in determining the emulsifying power of starch.
395 The highest proportion of OSA in food-grade products allowed by FDA is 3% (DS ~
396 0.023). All unhydrolyzed OSA-starches prepared here are at or below this limit.
397 Those samples hydrolyzed by *β*-amylase had an increased DS with increased enzyme
398 concentration (Fig. 4b), consistent with a previous report that the octenyl succinate
399 group can protect the grafting point from degrading (Sweedman, Tizzotti et al., 2013).
400 The higher range of DS is preferred for emulsification (Sweedman, Hasjim et al.,
401 2013). Although the DS increased, this increase is small because of residual small

402 molecules such as maltose, which contribute marked reducing end signals in the NMR
403 spectra (Fig. S1). The DS values of *α*-amylolysis samples were only slightly changed
404 because *α*-amylase only cuts (1→4)-α bonds, and thus it is not easy to remove octenyl
405 succinate groups in the hydrolysis process (Fig. 4a). As stated earlier, acid hydrolysis
406 works randomly through the starch granule, and the octenyl succinate groups, which
407 are mainly grafted on the surface of granule, can be removed easily. In addition, some
408 small molecules containing the octenyl succinate groups soluble in water and/or
409 ethanol might be removed during washing process with water and ethanol during the
410 preparation of the acid-hydrolyzed OSA-starch samples. This is why the acid-
411 hydrolyzed OSA-starches showed a clear decrease of DS with increasing hydrolysis
412 time (Fig. 4c). The relationships between the DS and functional properties are
413 discussed later.

414 ***3.2.* Functional properties of the hydrolyzed OSA-starch samples**

415 *3.2.1. Apparent viscosity*

416 Suspensions of OSA-starches usually have lower viscosities than native starches
417 because the process of synthesizing them results in some degradation. Low viscosity
418 is essential for some industrial operations, such as homogenizing and drying. As
419 shown in Fig. 5, all the hydrolyzed OSA-starch samples for all treatments showed a
420 decreasing tendency of apparent viscosity with increase of hydrolysis time,
421 particularly for the *α*-amylase hydrolyzed samples with the apparent viscosity

422 decreasing from ~3900 mPa·s (OS) to 25 mPa·s (A0.5) , consistent with their highest
423 extent of molecular degradation (Fig. 2 and Table 1). This suggests that the viscosities
424 of the OSA-starches are closely related with their molecular sizes. As shown in Fig.
425 5b for the *β*-amylase hydrolyzed samples, the viscosities were reduced remarkably
426 after a long hydrolysis time, which is mainly ascribed to the production of a large
427 fraction of maltose (Fig. 1b and Fig. 2b) (Zhang et al., 2018). Similar results were
428 observed for the acid-hydrolyzed samples. The viscosity of acid-hydrolyzed samples
429 reached a plateau after 3 h hydrolysis, corresponding to the plateau in average
430 molecular size after this time.

431 *3.2.2. Average droplet size of uncreamed layer of emulsion*

432 For all storage times after emulsification, the z-average emulsion droplet size for
433 the enzyme-hydrolyzed samples of the major phase of the emulsion (i.e. not the
434 creamed part) shows a similar trend with viscosity: decreasing with the increasing
435 hydrolysis time and thus decreasing average size (Fig. 6a and Fig. 6b), suggesting that
436 the emulsion droplet size and viscosity can be adjusted to the desirable range with
437 appropriate conditions. For the OSA-starch samples treated by HCl (Fig. 6c), the
438 emulsion droplet size showed insignificant change when the hydrolysis time was less
439 than 12 h, consistent with the structural results that there were no significant changes
440 in the average whole molecular size (Fig. 1c) and average chain length (Fig. 2c)
441 among the samples of H3, H6 and H12. Generally, the droplet size was initially ~ 500

442 – 600 nm, and after intensive hydrolysis was ~ 200 nm (Fig. 6).

443 The droplet size of the major (uncreamed) component of the emulsions after
444 different hydrolysis times increased, but only slightly (by ~ 10 – 50 nm), with an
445 increase of the storage time. The change in the droplet size during storage is believed
446 to be related to the modification of the surface adsorption capacity and the molecular
447 dispersion density of the OSA-starch. During the storage, a film is thought to form at
448 the emulsifier/droplet interface becomes thicker, resulting in increased particle size
449 (Qian, Decker, Xiao, & McClements, 2011). For the long-time acid hydrolysis
450 samples, the emulsion droplet size could not be tested due to the significant gelation
451 after emulsification (Fig. 6c). More information regarding the emulsion creaming is
452 discussed a later section.

453 *3.2.3. Emulsion stability*

454 The emulsion stability (%) of the major (uncreamed) component of the emulsion
455 is expressed by the change (%) in the droplet size of the emulsions over storage with
456 respect to the droplet size of the fresh emulsion (immediately after preparation).
457 Similarly, the creaming extent (%) is displayed by the creaming ratio of the height of
458 the creamed layer at the top of the centrifuge tube to the total height of the emulsion
459 sample at t=168 h. Droplet coalescence induced by the creaming may be formed
460 resulting in the instability of the emulsions. For the α-amylase hydrolyzed OSA-starch

461 samples (Fig. 6a and Table 1), there was a slight increase in the droplet size of the
462 emulsion after 2 days of storage (generally increased by ~ 5%, correspondingly to
463 0.1% per hour). With the increase of storage time to one week, the droplet size
464 increased by 10% (correspondingly to 0.06% per hour) at most compared to the
465 corresponding droplet size at the initial stage of storage. The emulsion droplet size of
466 the *β*-amylase hydrolyzed OSA-starch samples increased at a significantly faster rate
467 (the droplet size was increased by up to 40% after 168 h storage, correspondingly to
468 0.5% per hour) compared to those of the *α*-amylase hydrolyzed samples (Fig. 6b and
469 Table 1). The droplet size of the acid-hydrolyzed samples also increased significantly
470 over storage time and creaming occurred after a few hours' storage. Compared to the
471 emulsions prepared with the *β*-amylase and acid treatments, the emulsions of the *α*-
472 amylase hydrolyzed samples presented a relatively steady droplet size with the
473 increasing storage time indicting a better emulsion stability.

474 Even though the change of droplets size might be slight but the creaming or
475 gelation is significant, the emulsifier capacity is limited. Creaming was obvious after
476 a few hours' storage for the *β*-amylase and acid-hydrolyzed OSA-starch samples but
477 was not so significant for the samples treated by *α*-amylase. As shown in Fig. 7, the
478 creaming extent for all the emulsion samples significantly increased after 48 h storage
479 time but was significantly lower during storage for the OSA-starch samples treated by
480 *α*-amylase (lower than 7%) compared to those treated by *β*-amylase (up to 14%) and

481 HCl (up to 33%). A significant and positive correlation between the creaming extent
482 and the change in the emulsion droplet size over storage was observed (Table 1),
483 indicating a better emulsion stability for the emulsion samples with lower creaming
484 extent. As the emulsion droplet size was measured just for the uncreamed layer, the
485 increased droplet size shown here was perhaps due to the aggregation of short
486 branches after absorbing large amount of water, as this is the strongest difference
487 between the samples from the different preparation methods; the general principles of
488 colloidal stabilization show that short hydrophilic chains are less effective stabilizers
489 than long ones, all other things being equal (Napper, 1983). As such, the best
490 stabilizers, i.e. those which have the smallest change in the z-average droplet size and
491 smallest creaming extent over storage are those obtained using α-amylase hydrolyzed
492 OSA-starch samples with larger extent of molecular structure degradation such as the
493 samples of A3 and A4. In general, emulsions with better stability are preferable in
494 processed products in the food industry.

495 *3.2.4. Total antioxidant capacity*

496 The total antioxidant capacity (TAC) expressed by $FeSO_4$ concentration for the
497 OSA-starch samples with α-amylase, β-amylase and HCl treatments is shown in Fig.
498 8. The TAC measures the antioxidant capacity of OSA-starches. For the non-
499 hydrolyzed OSA-starch (OS), the $FeSO_4$ concentration was too low to be detected by
500 the ferric reducing antioxidant power (FRAP) assay, indicating negligible TAC for the

OS and the data was thus not included in Fig. 8. The acid hydrolysis of samples showed much better antioxidant capacity than the other two groups (Fig. 8). The amount of residual oxygen during the OSA-starch preparation and the hydrolyzing process is expected to be the same for all samples, because of similar procedures. Hence the different TAC is ascribed to more long branch chains (Fig. 2c) with more reducing end groups in the acid-hydrolyzed samples. The TAC of β-amylase hydrolyzed samples was slightly higher than the α-amylase hydrolyzed samples, probably attributed from the larger amount of maltose fractions with more reducing end groups in the samples with β-amylase treatment (Fig. 1b). In addition, the TAC of all the OSA-starches generally remained unchanged over the hydrolysis time, indicating the hydrolysis time was not the dominant role in determining their TAC.

3.3. Correlations between structural and functional properties

The structural parameters of importance considered here are average molecular size of the whole molecule ($\overline{R_h}$), average chain length ($\overline{DP}$), degree of branching (DB) and degree of substitution (DS). The functional properties against which structure-property correlations are sought are initial and stored droplet size, emulsification stability (%) as measured by the change of droplet size with storage time, viscosity, extent of creaming and TAC of the hydrolyzed OSA-starch samples. The Pearson's and Spearman's rank correlation coefficients of structure-structure and structure-

property for all the tested samples irrespective of preparation approaches are given in Table 2. The correlations in consideration of the preparation approach are presented in Table S1 of Supporting Information, which generally indicated similar correlation results with those shown in Table 2. Overall, most of the coefficients obtained from the Pearson's and Spearman's rank correlations are similar to each other, except that several correlations are different, i.e. the correlations between the $\bar{X}$ /DB and TAC are significant obtained from the Pearson method whereas they were statistically indifferent obtained from the Spearman method. The different correlations are attributed from the fact that the Pearson's correlation test detects linear relations, while Spearman's rank correlation test is also able to reveal non-linear relations. Independent of the correlation analyzing method, the two structural parameters, $\bar{X}$ and $\overline{R_{\mathrm{h}}}$, are always significantly and positively correlated with each other, and both showed significant and negative correlations with DB.

Table 2. Pearson (P) and Spearman (S) correlation coefficients of structure-structure and structure-property for all the tested samples irrespective of preparation approach [1].

Correlation coefficients		Structural parameters								Functional parameters															
		$\overline{R_h}$		$\bar{X}$		DB		DS		TAC		Viscosity		Creaming extent		z-average droplet size						Droplet stability			
																0 h		48 h		168 h		48 h		168 h	
		P	S	P	S	P	S	P	S	P	S	P	S	P	S	P	S	P	S	P	S	P	S	P	S
$\bar{X}$		0.86**	0.92**																						
DB		-0.76**	-0.86**	-0.89**	-0.91**																				
DS		0.30	0.05	-0.06	-0.01	-0.50*	-0.15																		
TAC		0.36	0.16	0.67**	0.40	-0.48*	-0.36	-0.36	0.13																
Viscosity		0.79**	0.90**	0.62*	0.90**	-0.65**	-0.94**	0.57*	0.23	0.12	0.22														
Creaming		0.34	0.37	0.58*	0.62**	-0.62**	-0.59*	0.04	0.10	0.75**	0.86**	0.34	0.51*												
z-average droplet size	0 h	0.78**	0.82**	0.75**	0.78**	-0.59**	-0.64**	0.17	-0.02	0.42	-0.02	0.46	0.68**	0.19	0.15										
	48 h	0.79**	0.88**	0.80**	0.84**	-0.65**	-0.69**	0.16	0.04	0.47	0.05	0.47	0.76**	0.29	0.26	0.99**	0.98**								
	168 h	0.78**	0.90**	0.80**	0.88**	-0.66**	-0.73**	0.12	0.03	0.49*	0.09	0.46	0.79**	0.31	0.31	0.98**	0.96**	0.99**	0.99**						
Droplet stability	48 h	-0.20	-0.12	0.04	0.01	-0.18	-0.06	-0.15	0.23	0.22	0.35	-0.10	0.10	0.59**	0.53*	-0.40	-0.42	-0.27	-0.28	-0.24	-0.27				
	168 h	-0.07	0.02	0.20	0.15	-0.32	-0.22	-0.32	0.18	0.37	0.55*	-0.06	0.20	0.63**	0.69**	-0.26	-0.33	-0.14	-0.19	-0.07	-0.14	0.88**	0.81**		

[1] *. Correlation is significant at the 0.05 level (2-tailed)

**. Correlation is significant at the 0.01 level (2-tailed)

3.3.1. Structure-viscosity relations

As shown in Table 2, the average whole molecular size $\overline{R_h}$ and the average chain length $\bar{X}$ both have a significantly positive correlation with the apparent viscosity of all the hydrolyzed OSA-starch samples independent of hydrolysis approaches. This suggests that the viscosity of the hydrolyzed OSA-starch solution could be adjusted by the treatment of the three hydrolysis approaches. With increasing hydrolysis time of the OSA-starches, the proportion of long amylopectin (DP X ~56, shown in Fig. 2) chains became less while that of short chains increased, and the number of branch points also increased, thus causing the reduced viscosity and negative correlation between the two structural parameters ($\overline{R_h}$ and $\bar{X}$) of the hydrolysates and the viscosity. The reasons for these effects are well understood in terms of the rheology of polymer solutions.

DB negatively correlates with viscosity. High DB means fewer long chains. This correlation can be ascribed to the well-known effects of longer polymer chains in solution on viscosity: a given mass of long chains in solution will have a much greater impediment to flow than the same mass of shorter ones (think of longer chains entangling around a rod being dragged through the polymer solution). Samples with high DS tend to have higher viscosity. Although DB and DS are not the dominant reasons to determine the viscosity, when the molecular size and components are similar these secondary structures can play a significant role in the viscosity. A higher

559 DS means more hydrophilic groups, which can make aggregates (polydisperse
560 micelles), resulting in the increase of viscosity. A high DS would also result in more
561 charged succinate groups (or very hydrophilic succinic acid groups, if low pH), which
562 would result in more tightly bound water molecules causing higher viscosity (Miao et
563 al., 2014; Sweedman, Hasjim et al., 2014).

564 *3.3.2. Structure-creaming extent relations*

565 The creaming extent is a very important indicator of emulsion stability, with lower
566 creaming extent indicating better stability as stated previously (Table 2). The $\bar{X}$ and
567 DB showed significantly positive and negative correlations with the creaming extent,
568 respectively, for all the tested samples irrespective of hydrolysis approach. This
569 indicates that the longer hydrolyzing time which resulted in relatively shorter branch
570 chains and more branching points tended to produce more stable emulsion with lower
571 creaming extent due to the steric hindrance effect and electrostatic repulsion from the
572 carboxylate groups (Sweedman, Hasjim et al., 2014; Sweedman, Hasjim et al., 2013).
573 Compared to the acid-hydrolyzed OSA samples, the samples treated with α-amylase
574 and β-amylase in general had smaller $\bar{X}$ and larger DB, resulting in better emulsion
575 stability with lower creaming extent. However, statistically inconsistent correlations
576 were observed within groups due to the big differences in the values of $\bar{X}$ and
577 creaming extent between the samples hydrolyzed by enzymes and HCl. For example,
578 as shown in Table S1, there are no significant correlations between the $\bar{X}$ and

579 creaming extent for the OSA-starch samples hydrolyzed by α-amylase and β-amylase.
580 Besides, the $\bar{X}$ or $\overline{R_h}$ showed significantly negative correlation with the creaming
581 extent for the acid-hydrolyzed samples (Table S1), due to the coalescence of many
582 small molecules with short chains during the storage period causing the increasing
583 creaming with the decrease of $\bar{X}$ or $\overline{R_h}$ (Sweedman, Schafer, & Gilbert, 2014).
584 Similarly, significant correlations between the DS/DB and creaming extent were
585 observed for the acid-hydrolyzed samples whereas these were not shown for the OSA-
586 starch samples hydrolyzed by α-amylase and β-amylase. These inconsistent structure-
587 creaming extent correlations between the enzyme and acid-hydrolyzed samples
588 indicate that the emulsion creaming extent was closely related with the hydrolysis
589 approach for the OSA-starches. Hence, the method of OSA-starch hydrolysis should
590 be taken into account when preparing emulsifiers with desired functional properties.

591 *3.3.3. Structure-droplet size relations*

592 The emulsion droplet size positively and significantly correlated with $\overline{R_h}$ and $\bar{X}$ of
593 all hydrolysates, independent of the storage time and hydrolysis approach (Table 2
594 and Table S1). The droplet size increasing with size and chain length of the emulsifier
595 (larger $\overline{R_h}$ and $\bar{X}$) can be understood when it is recalled that all emulsions had the
596 same mass of emulsifier, and thus if the emulsifier molecules are larger (larger $\overline{R_h}$ and
597 $\bar{X}$) then the number of emulsifier molecules will be smaller, and thus there will be less
598 of them to cover the droplet surface, causing less effective stabilization and thus

599 larger droplets, all other things being equal. In addition, the emulsion droplet size was
600 negatively and strongly correlated with the DB for the hydrolyzed OSA-starches,
601 suggesting that the OSA-starch with more branches can form smaller size of
602 emulsions. There is no significant correlation between the DS and droplet size.

603 *3.3.4. Structure-droplet stability relations*

604 It has been reported that longer branching chains and more branches contribute to
605 more stable droplet size for OSA-starch emulsions (Sweedman, Tizzotti et al., 2013;
606 Wang, Su, & Wang, 2010). This can be explained by the effect of steric hindrance that
607 can be created easily as there are many branches and long chains. However, as shown
608 in this study all the structural parameters don't display significant correlation with the
609 droplet stability of the emulsion probably due to varying manufacturing process for
610 the OSA-starches. This may indicate that the molecular structure of the OSA-starch is
611 not the dominant role in determining the droplet stability of the emulsions. The
612 droplet size and viscosity are well correlated with the structural features, suggesting
613 that longer hydrolysis time can produce smaller stabilizer molecules with lower
614 viscosity, but cannot ensure good performance of the emulsion stability. Therefore, an
615 optimal condition of hydrolysis is necessary.

616 *3.3.5. Structure-total antioxidant capacity relations*

617 The relationships between the structural parameters and antioxidant capacity are

618 complex, because the antioxidant capacity is sensitive to many environmental factors.
619 The $\bar{X}$ and DB showed strongly positive and negative correlations with the total
620 antioxidant capacity (TAC), respectively. The TAC is closely related to the amount of
621 reducing end groups present in the sample. After hydrolysis, some reducing sugars
622 such as maltose and dextrin fractions were released causing the increase of the TAC.
623 But it should be noted that the amount of non-reducing end groups associated with
624 DB also increased after hydrolysis. The α-amylase hydrolyzed OSA-starch samples
625 mostly had the highest DB thereby causing the production of the largest amount of
626 non-reducing ends. Accordingly, the proportion of the reducing end groups was the
627 lowest, consistent with their lowest TAC. The acid-hydrolyzed OSA samples had
628 larger $\bar{X}$ and smaller DB compared to the enzyme-treated samples, resulting in better
629 TAC. In addition, the creaming extent is strongly correlated with the TAC, which
630 indicates that the emulsion stability and TAC might be contradictory to each other.
631 The acid treatment on the OSA samples can produce hydrolysates with good TAC but
632 bad emulsion stability meanwhile. The DS is negatively correlated with the TAC
633 although the correlation was not statistically significant. This may indicate that the
634 TAC of the OSA-starch samples was affected by their DS to some extent.

635

636 ## 4. Conclusions

637 In this study, the OSA-starches were prepared and the structural and functional
638 properties of the OSA-starches with the α-amylase, β-amylase and HCl hydrolysis for
639 varying times were evaluated. With the increase of hydrolysis time, the average whole
640 molecular size and average chain length for all the OSA-starch samples with varying
641 treatments were significantly decreased indicating the molecular degradation due to
642 the enzyme or acid hydrolysis. Correspondingly, the DB and DS were slightly
643 increased and decreased over time, respectively. The different hydrolysis approaches
644 could result in the structural and functional differences among the OSA-starch
645 samples due to the variations in steric hindrance effect and electrostatic repulsion
646 from the carboxylate groups. The samples after being intensively hydrolyzed by β-
647 amylase had a large amount of maltose fractions, resulting in low apparent viscosity
648 and small emulsion droplet size. The α-amylase hydrolyzed samples presented the
649 best emulsion stability with the lowest creaming extent compared to the OSA-starch
650 samples with β-amylase and HCl treatments. The acid-treated samples showed largest
651 emulsion droplet size but the worst emulsion stability probably due to the aggregation
652 of short branching chains and the gelation after absorbing large amount of water,
653 whereas the best total antioxidant capacity. The observed structure-property
654 correlations indicate that the chain length and DB are the two key factors determining
655 the apparent viscosity, TAC, and emulsion droplet size and creaming extent of the
656 OSA-starches. These findings indicate the possible approaches to improving the

657 performances of OSA-starches used as emulsifier in food industry.

658 Acknowledgements

659 We gratefully acknowledge the DSM Nutritional Products and the National
660 Science Foundation of China (grant C130401 3151101138) for funding. We thank Mr
661 Shiqing Zhou (Polysaccharide Research Centre, Wuhan, China) for SEC data
662 processing.

663 References

664 Benzie, I. F. F., & Strain, J. J. (1996). The Ferric Reducing Ability of Plasma (FRAP) as a
665 Measure of "Antioxidant Power": The FRAP Assay. *Analytical Biochemistry, 239*(1), 70-
666 76.
667 Cave, R. A., Seabrook, S. A., Gidley, M. J., & Gilbert, R. G. (2009). Characterization of Starch by
668 Size-Exclusion Chromatography: The Limitations Imposed by Shear Scission.
669 *Biomacromolecules, 10*(8), 2245-2253.
670 Dhital, S., Warren, F. J., Butterworth, P. J., Ellis, P. R., & Gidley, M. J. (2017). Mechanisms of
671 starch digestion by α-amylase–structural basis for kinetic properties. *Critical Reviews in*
672 *Food Science and Nutrition, 57*(5), 875-892.
673 Dokic, P., Dokic, L., Dapcevic, T., & Krstonosic, V. (2008). Colloid Characteristics and
674 Emulsifying Properties of OSA Starches. In Z. D. Horvolgyi & E. Kiss (Eds.), *Colloids*
675 *for Nano- and Biotechnology* (Vol. 135). Heidelberg: Springer-Verlag.
676 Hamaker, B. R., Lee, B.-H., & Quezada-Calvillo, R. (2012). Starch Digestion and Patients With
677 Congenital Sucrase-Isomaltase Deficiency. *Journal of Pediatric Gastroenterology and*
678 *Nutrition, 55*, S24-S28.
679 Hategekimana, J., Masamba, K. G., Ma, J., & Zhong, F. (2015). Encapsulation of vitamin E:
680 Effect of physicochemical properties of wall material on retention and stability.
681 *Carbohydrate Polymers, 124*, 172-179.
682 Hoover, R. (2000). Acid-treated starches. *Food Reviews International, 16*(3), 369-392.
683 LeCorre, D., Vahanian, E., Dufresne, A., & Bras, J. (2012). Enzymatic Pretreatment for Preparing
684 Starch Nanocrystals. *Biomacromolecules, 13*(1), 132-137.
685 Lin, J.-H., Lee, S.-Y., & Chang, Y.-H. (2003). Effect of acid–alcohol treatment on the molecular
686 structure and physicochemical properties of maize and potato starches. *Carbohydr*
687 *Polymers, 53*(4), 475-482.
688 Liu, Z., Li, Y., Cui, F., Ping, L., Song, J., Ravee, Y., Jin, L., Xue, Y., Xu, J., Li, G., Wang, Y., &

689 Zheng, Y. (2008). Production of Octenyl Succinic Anhydride-Modified Waxy Corn Starch
690 and Its Characterization. *Journal of Agricultural and Food Chemistry, 56*(23), 11499-
691 11506.
692 Luo, J., Li, L., & Kong, L. (2012). Preparative separation of phenylpropenoid glycerides from the
693 bulbs of Lilium lancifolium by high-speed counter-current chromatography and
694 evaluation of their antioxidant activities. *Food Chemistry, 131*(3), 1056-1062.
695 Ma, W.-P., & Robyt, J. F. (1987). Preparation and characterization of soluble starches having
696 different molecular sizes and composition, by acid hydrolysis in different alcohols.
697 *Carbohydrate Research, 166*(2), 283-297.
698 Miao, M., Li, R., Huang, C., Jiang, B., & Zhang, T. (2015). Impact of beta-amylase degradation on
699 properties of sugary maize soluble starch particles. *Food Chemistry, 177*, 1-7.
700 Miao, M., Li, R., Jiang, B., Cui, S. W., Lu, K. Y., & Zhang, T. (2014). Structure and digestibility of
701 endosperm water-soluble alpha-glucans from different sugary maize mutants. *Food*
702 *Chemistry, 143*, 156-162.
703 Modig, G., Nilsson, L., Bergenståhl, B., & Wahlund, K. G. (2006). Homogenization-induced
704 degradation of hydrophobically modified starch determined by asymmetrical flow field-
705 flow fractionation and multi-angle light scattering. *Food Hydrocolloids, 20*(7), 1087-
706 1095.
707 Mortenson, M. A., & Reineccius, G. A. (2008). Encapsulation and release of menthol. Part 1: the
708 influence of OSAn modification of carriers on the encapsulation of l□menthol by spray
709 drying. *Flavour & Fragrance Journal, 23*(6), 392–397.
710 Napper, D. H. (1983). *Polymeric stabilization of colloidal dispersions*. London: Academic.
711 Nilsson, L., & Bergenståhl, B. (2006). Adsorption of hydrophobically modified starch at oil/water
712 interfaces during emulsification. *Langmuir, 22*(21), 8770-8776.
713 Nilsson, L., & Bergenståhl, B. (2007). Emulsification and adsorption properties of
714 hydrophobically modified potato and barley starch. *Journal of Agricultural and Food*
715 *Chemistry, 55*(4), 1469-1474.
716 Park, S., Chung, M.-G., & Yoo, B. (2004). Effect of Octenylsuccinylation on Rheological
717 Properties of Corn Starch Pastes. *Starch - Stärke, 56*(9), 399-406.
718 Qian, C., Decker, E. A., Xiao, H., & McClements, D. J. (2011). Comparison of biopolymer
719 emulsifier performance in formation and stabilization of orange oil-in-water emulsions.
720 *Journal of the American Oil Chemists' Society, 88*(1), 47-55.
721 Robyt, J. F., Choe, J.-y., Hahn, R. S., & Fuchs, E. B. (1996). Acid modification of starch granules
722 in alcohols: effects of temperature, acid concentration, and starch concentration.
723 *Carbohydrate Research, 281*(2), 203-218.
724 Stang, M., Schuchmann, H., & Schubert, H. (2001). Emulsification in High-Pressure
725 Homogenizers. *Engineering in Life Sciences, 1*(4), 151–157.
726 Sweedman, M. C., Hasjim, J., Shaefer, C., & Gilbert, R. G. (2014). Structures of octenyl
727 succinylated starches: Effects on emulsions containing beta-carotene. *Carbohydrate*
728 *Polymers, 112*(1), 85-93.

Sweedman, M. C., Hasjim, J., Tizzotti, M. J., Schaefer, C., & Gilbert, R. G. (2013). Effect of octenylsuccinic anhydride modification on beta-amylolysis of starch. *Carbohydrate Polymers, 97*(1), 9-17.

Sweedman, M. C., Schaeffer, C., & Gilbert, R. G. (2014). Aggregate and emulsion properties of enzymatically-modified octenyl succinylated waxy starches. *Carbohydrate Polymers, 111*(1), 918-927.

Sweedman, M. C., Tizzotti, M. J., Schafer, C., & Gilbert, R. G. (2013). Structure and physicochemical properties of octenyl succinic anhydride modified starches: A review. *Carbohydrate Polymers, 92*(1), 905-920.

Tesch, S., Gerhards, C., & Schubert, H. (2002). Stabilization of emulsions by OSA starches. *Journal of Food Engineering, 54*(2), 167-174.

Tizzotti, M. J., Sweedman, M. C., Schaefer, C., & Gilbert, R. G. (2013). The influence of macromolecular architecture on the critical aggregation concentration of large amphiphilic starch derivatives. *Food Hydrocolloids, 31*(2), 365-374.

Tizzotti, M. J., Sweedman, M. C., Tang, D., Schaeffer, C., & Gilbert, R. G. (2011). New 1H NMR Procedure for the Characterization of Native and Modified Food-Grade Starches. *Journal of Agricultural and Food Chemistry, 59*(13), 6913-6919.

Tran, T. T. B., Shelat, K. J., Tang, D., Li, E., Gilbert, R. G., & Hasjim, J. (2011). Milling of rice grains: the degradation on three structural levels of starch can be independently controlled during grinding. *Journal of Agricultural and Food Chemistry, 59*(8), 3964-3973.

Viksø-Nielsen, A., Andersen, C., Hoff, T., & Pedersen, S. (2006). Development of new α-amylases for raw starch hydrolysis. *Biocatalysis and Biotransformation, 24*(1-2), 121-127.

Vilaplana, F., & Gilbert, R. G. (2010a). Characterization of branched polysaccharides using multiple-detection size separation techniques. *Journal of Separation Science, 33*(22), 3537–3554.

Vilaplana, F., & Gilbert, R. G. (2010b). Two-dimensional size/branch length distributions of a branched polymer. *Macromolecules, 43*(17), 7321-7329.

Wang, J., Su, L., & Wang, S. (2010). Physicochemical properties of octenyl succinic anhydride-modified potato starch with different degrees of substitution. *Journal of the Science of Food and Agriculture, 90*(3), 424-429.

Wang, S., Blazek, J., Gilbert, E., & Copeland, L. (2012). New insights on the mechanism of acid degradation of pea starch. *Carbohydrate Polymers, 87*, 1941-1949.

Xu, Y. F., Huang, Q., Fu, X., & Jane, J. L. (2015). Modification of starch octenylsuccinate by beta-amylase hydrolysis in order to increase its emulsification properties. *Food Hydrocolloids, 48*, 55-61.

Zhang, H., Schäfer, C., Wu, P., Deng, B., Yang, G., Li, E., Gilbert, R. G., & Li, C. (2018). Mechanistic understanding of the relationships between molecular structure and emulsification properties of octenyl succinic anhydride (OSA) modified starches. *Food Hydrocolloids, 74*, 168-175.

Figure captions

Figure 1. SEC weight distributions of the whole OSA-starch samples after being hydrolyzed by *α*-amylase (a), *β*-amylase (b) and HCl (c) for different times. OSA starch samples after hydrolysis by *β*-amylase with low enzyme concentration for 0.5, 1, 2 and 4 h, with medium concentration for 2 h, and with high concentration for 0.5, 1 and 2 h, are denoted BL0.5, BL1, BL2, BL4, BM2, BH0.5, BH1 and BH2, respectively. Similarly, A0.5-A4 represent the OSA-starch samples after hydrolysis by *α*-amylase for time periods ranging from 0.5 to 4 h, H3-H336 represent the OSA-starch samples treated by 2.2 M HCl for the time periods ranging from 3 to 336 h.

Figure 2. SEC weight CLDs of debranched OSA-starches after being hydrolyzed by *α*-amylase (a), *β*-amylase (b) and HCl (c) for different times. The meanings of the sample codes are as described in **Figure 1**.

Figure 3. The DB of OSA-starches after being hydrolyzed by *α*-amylase (a), *β*-amylase (b), and HCl (c) for different times. OS represents non-hydrolyzed OSA-starch; sample codes are the same as shown in **Figure 1**.

Figure 4. The DS of OSA-starches after being hydrolyzed by *α*-amylase (a), *β*-amylase (b), and HCl (c) for different times. The sample code OS is non-hydrolyzed OSA-starch; other codes are as the same in **Figure 1**.

Figure 5. The viscosity of OSA-starches after hydrolysis by *α*-amylase (a), *β*-amylase (b), and HCl (c) for different times, measured at concentrations of 40% (w/w) in water at 50^{o}C. The meanings of the sample codes are the same as described in **Figure 1**.

Figure 6. The z-average droplet size of emulsions made with OSA-starches after being hydrolyzed by *α*-amylase (b), *β*-amylase (a), and HCl (c) for different times. Sample codes are as described in **Figure 1**.

Figure 7. The creaming extent (%) of the emulsions produced by hydrolyzing the OSA-starch samples with *α*-amylase (a), *β*-amylase (b) and HCl (c) at 168 h storage. The sample codes are as described in **Figure 1.**

Figure 8. The total antioxidant capacity (TAC) of OSA-starches after being hydrolyzed by *α*-

796 amylase, β-amylase, and HCl for different times. The meanings of the sample codes are as
797 described in **Figure 1**.

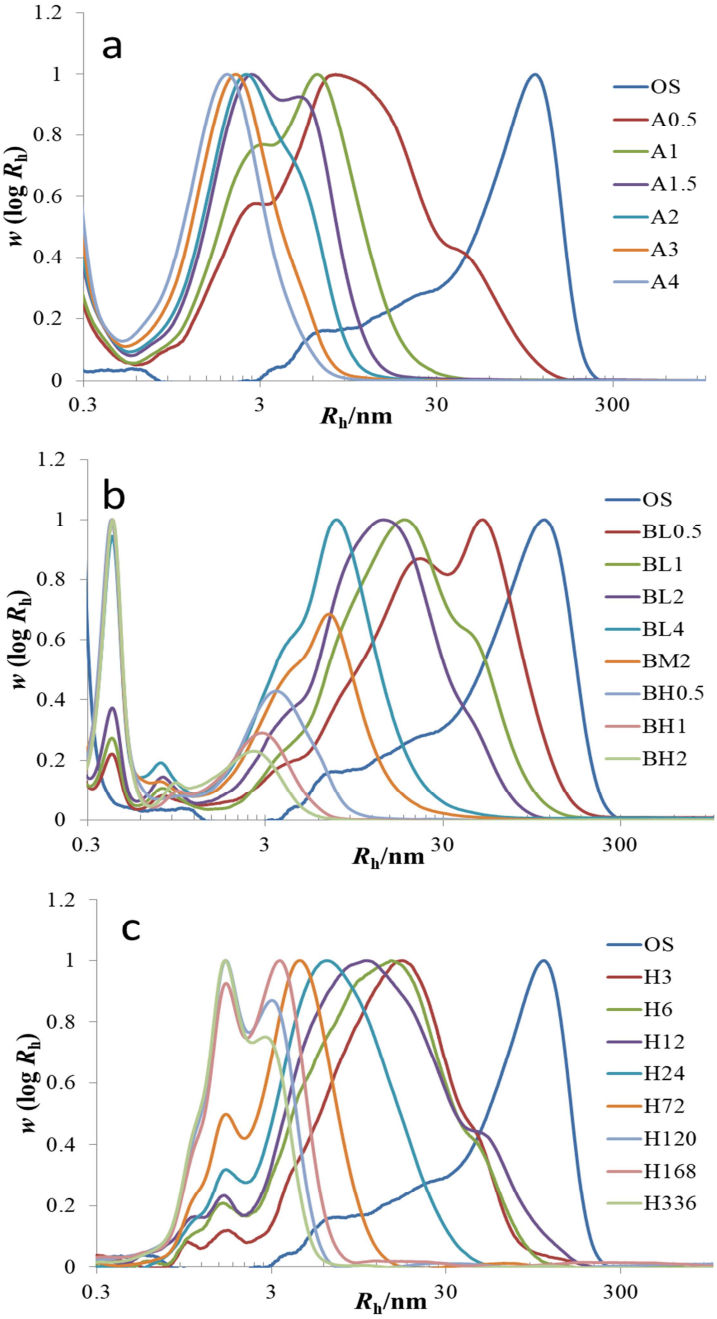

798

799 **Figure 1**

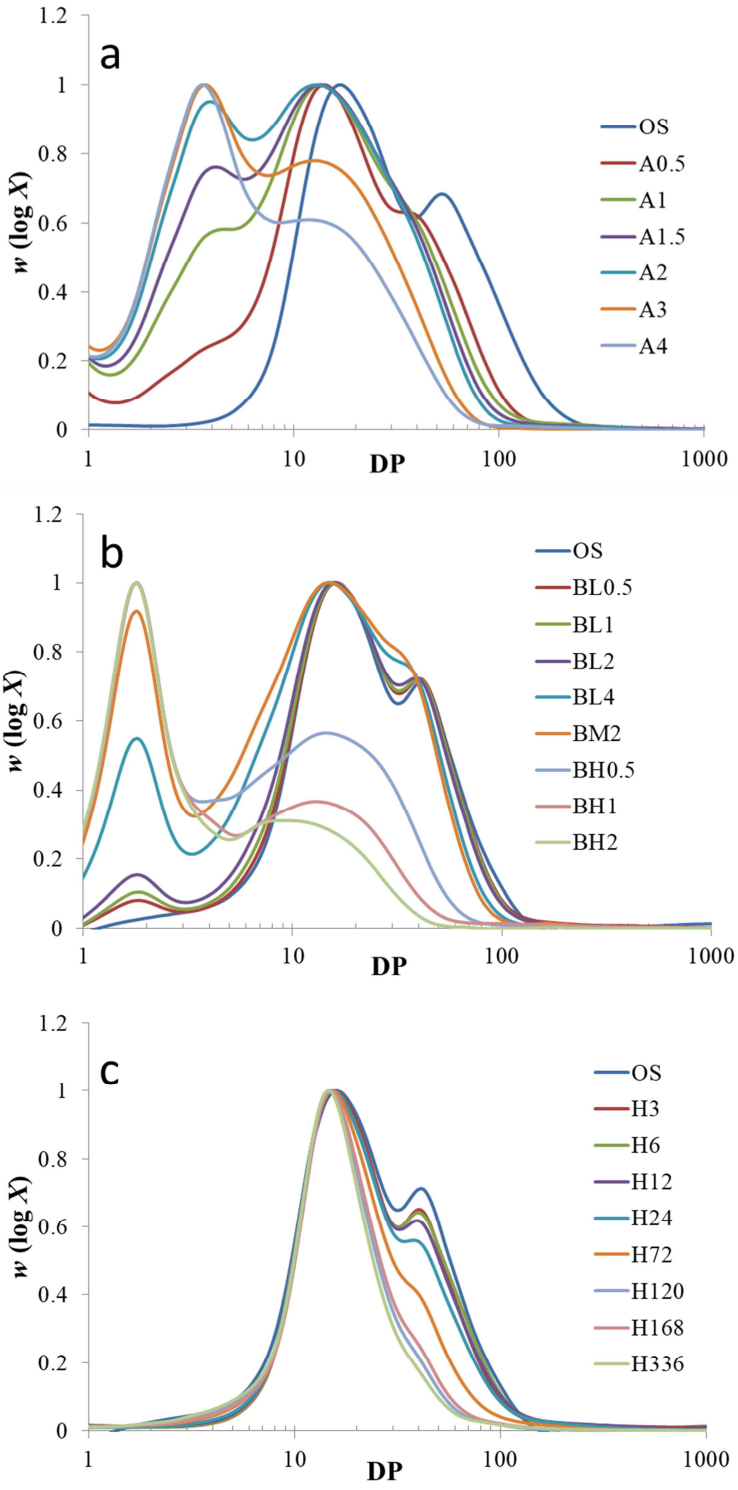
a
w (log X)
DP
OS
A0.5
A1
A1.5
A2
A3
A4
b
w (log X)
DP
OS
BL0.5
BL1
BL2
BL4
BM2
BH0.5
BH1
BH2
c
w (log X)
DP
OS
H3
H6
H12
H24
H72
H120
H168
H336

Figure 2

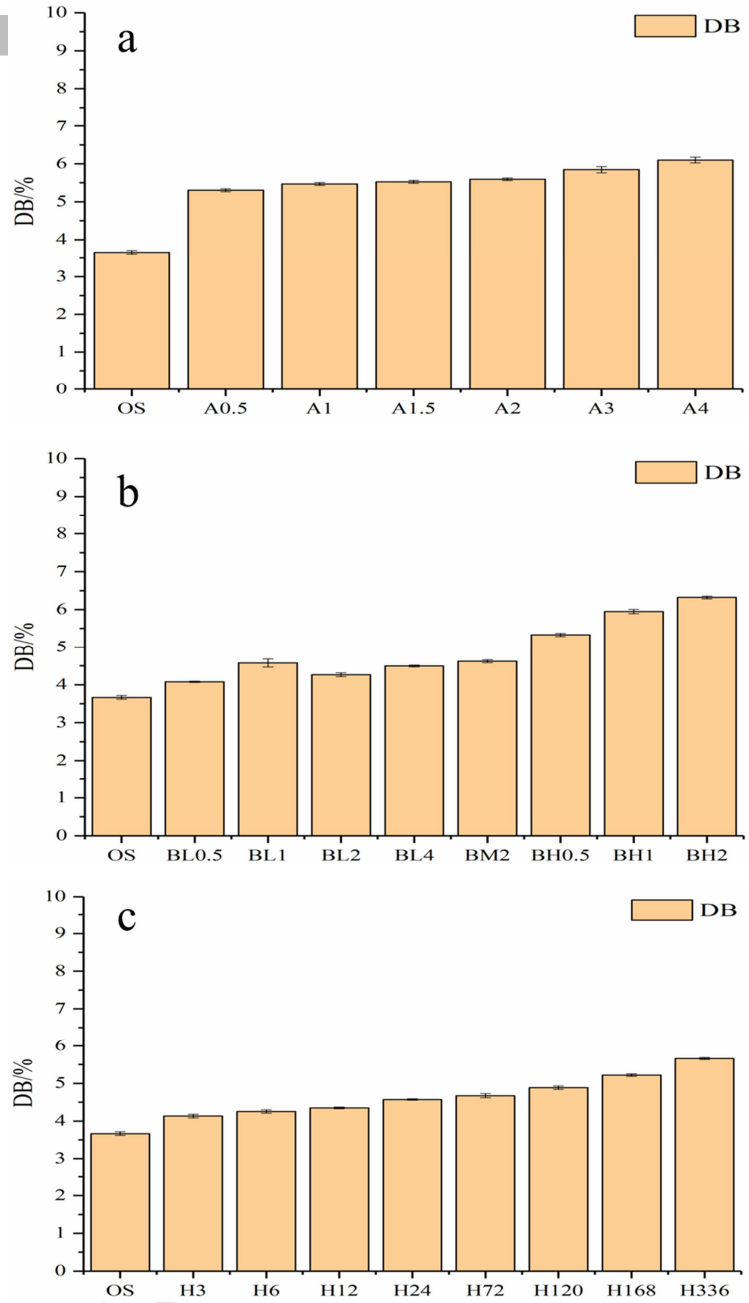

Figure 3

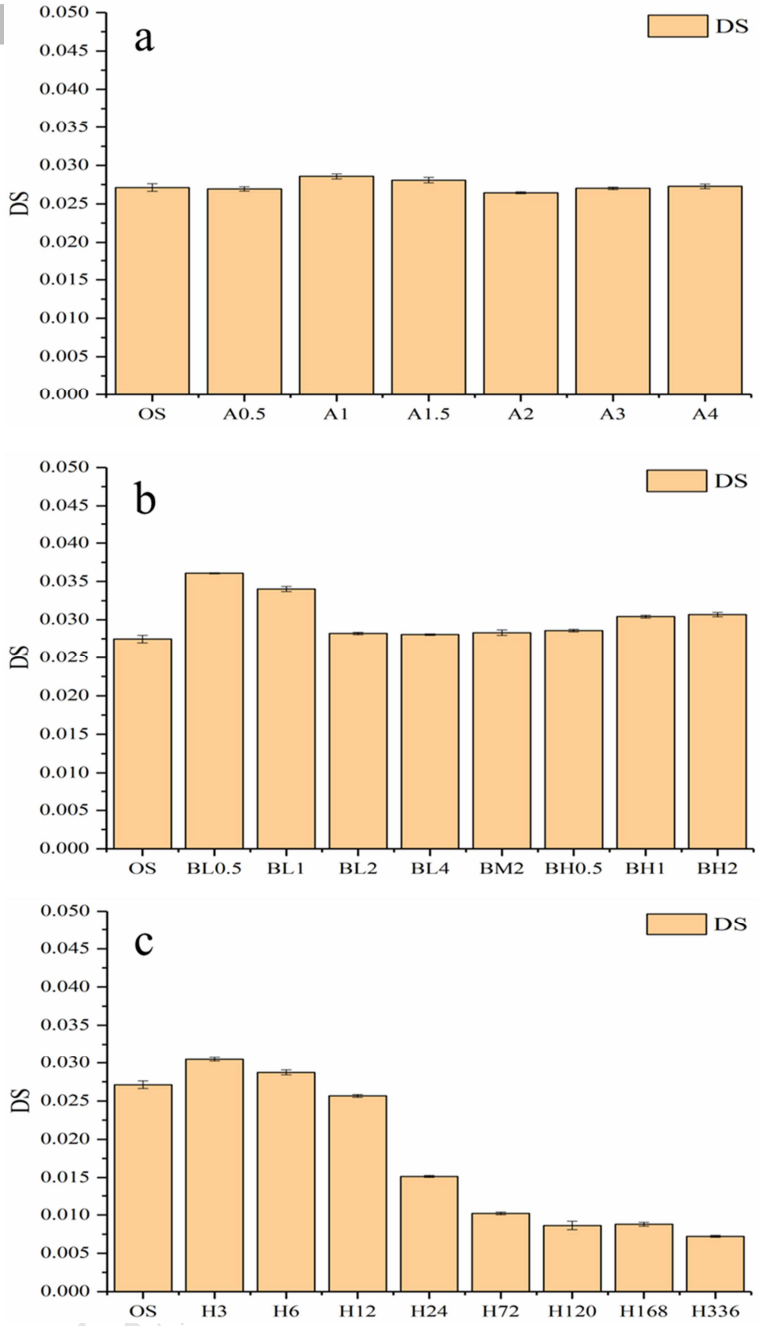

804

805 **Figure 4**

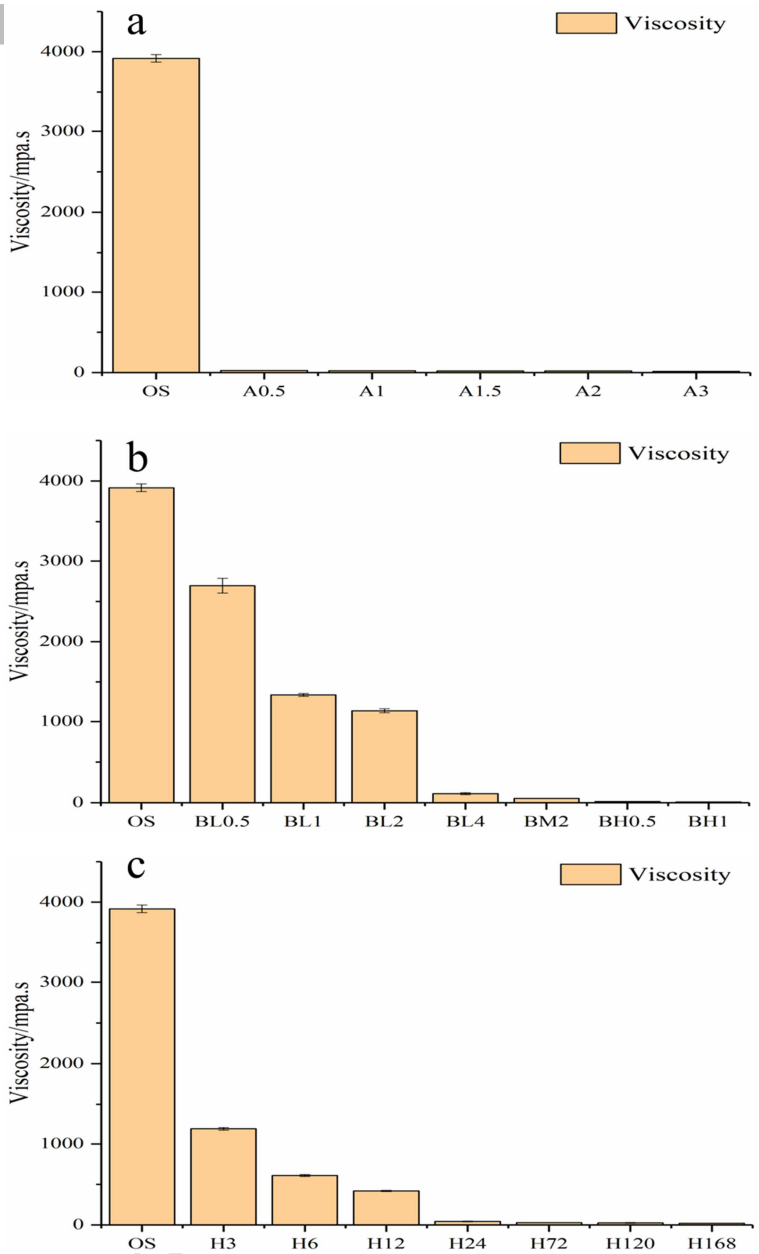

Figure 5

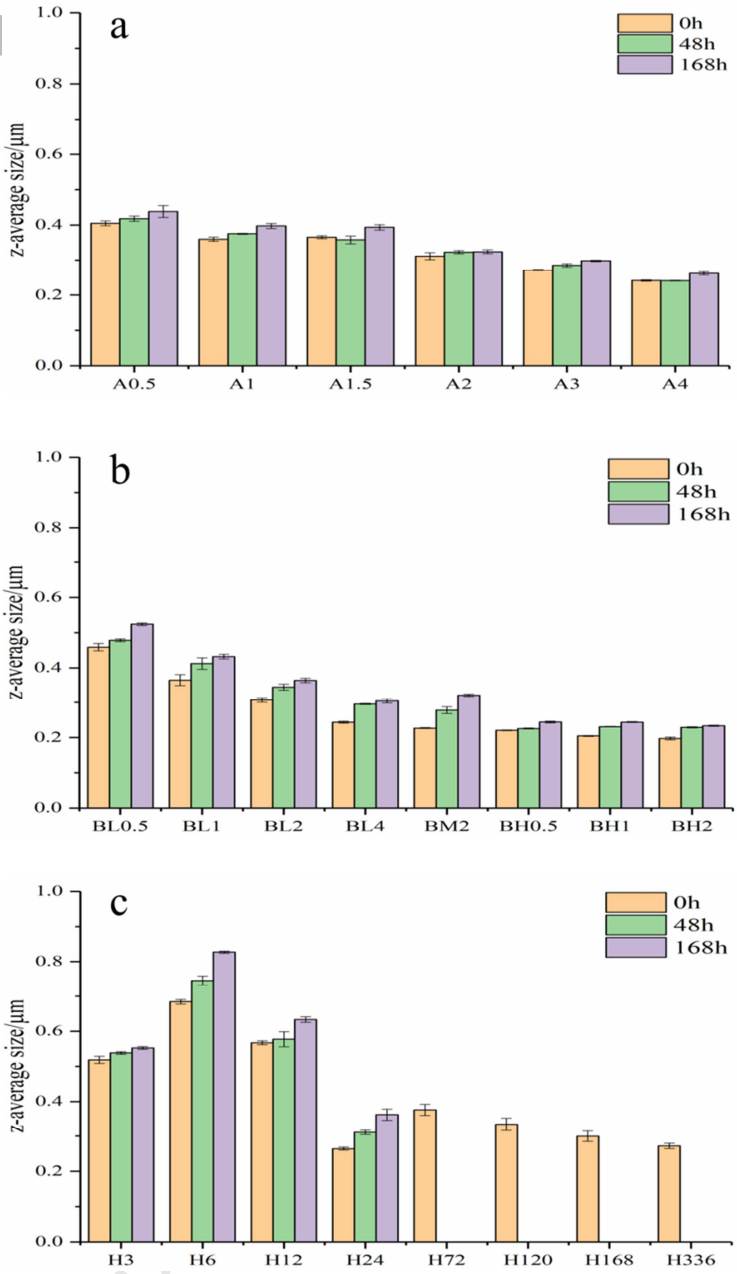

Figure 6

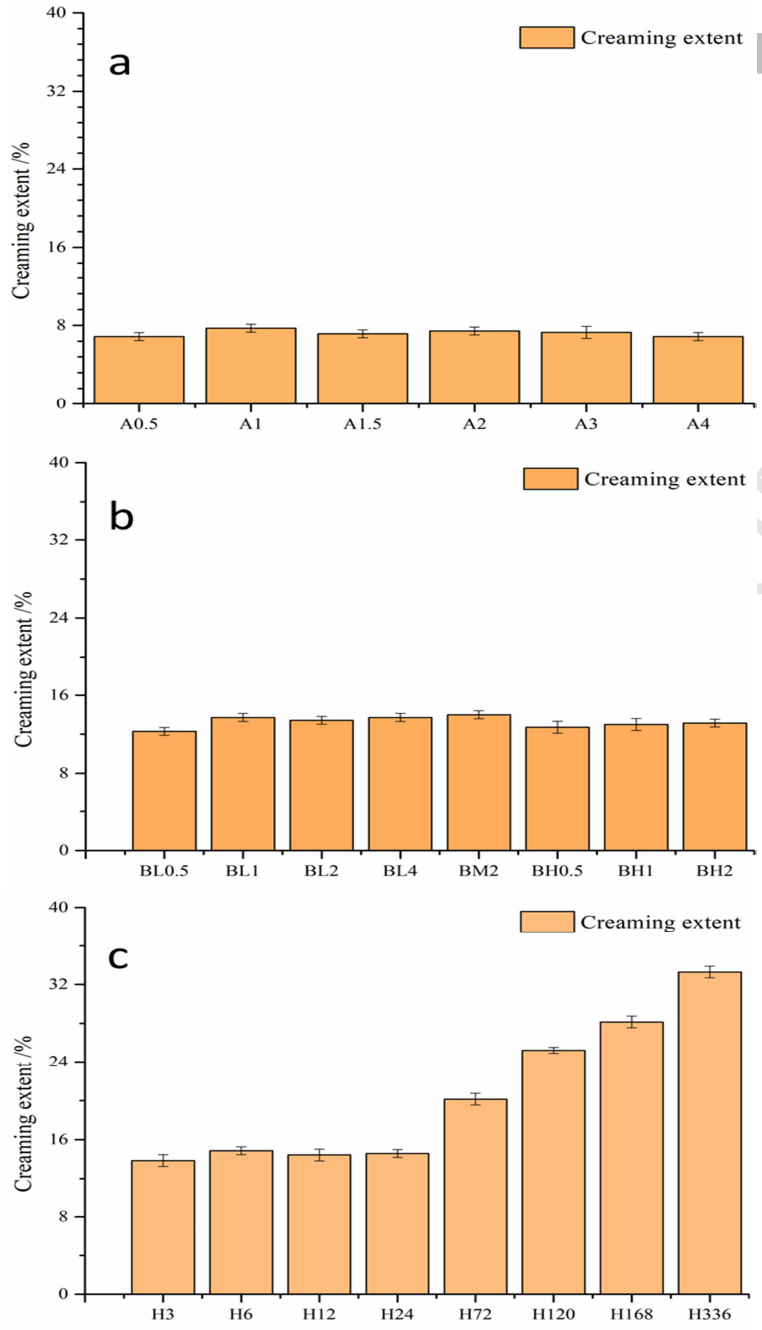

Figure 7

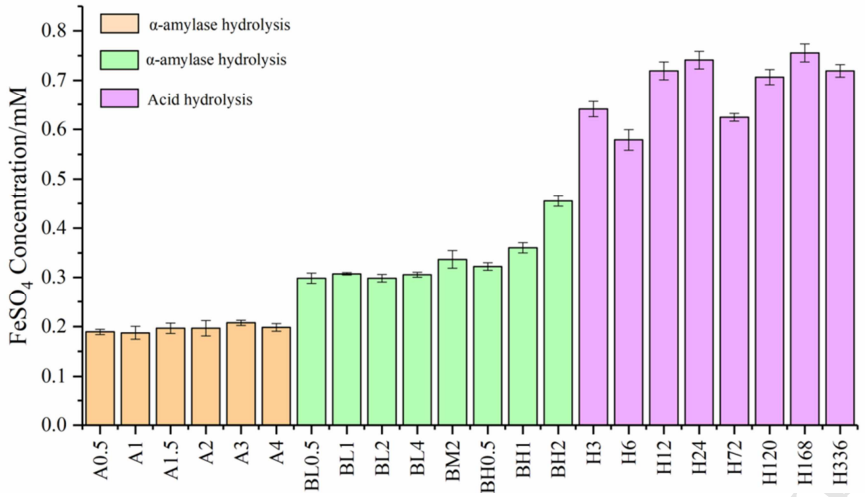

812

813 **Figure 8**

Highlights

- ~~A wide range of OSA-starches were hydrolyzed by amylase and HCl~~
- Average DP positively correlated with viscosity, TAC and emulsion droplet size
- ~~Molecular structures of hydrolyzed OSA-starch samples were characterized using SEC~~
- DP and DB of OSA-starches are the two key factors determining functional properties
- ~~Functional emulsification properties were measured and correlated with structures~~
- α-amylase-hydrolyzed OSA-starches had lowest viscosity and best droplet stability
- Acid-hydrolyzed OSA-starches presented better TAC while lower droplet stability
- *β*-amylase hydrolysis produced moderate structural degradation and emulsifying properties